Journal of Building Engineering 33 (2021) 101599

Contents lists available at ScienceDirect

Journal of Building Engineering

journal homepage: http://www.elsevier.com/locate/jobe

Analysis of thermal comfort in a football stadium designed for hot and humid climates by CFD

Gianluca Losi, Arianna Bonzanini, Andrea Aquino *, Pietro Poesio **

Department of Mechanical and Industrial Engineering, University of Brescia, Brescia, 25123, Italy

ARTICLE INFO

Keywords:
Stadium CFD analysis
Thermal comfort
Conjugate heat transfer
HVAC
Hot and humid climate conditions

ABSTRACT

Qatar is hosting the 2022 FIFA World Cup. In the field of sports architecture, this is a challenging case study for new design solutions that guarantee the comfort and safety of occupants in such a hot and humid climate. This work analyzes the thermal comfort of a stadium designed for international competitions in Doha, Qatar. The stadium has a total capacity of 47,000 spectators. An external façade protects the occupants from exposure to wind and sunlight, and fresh air and daylight enter the stadium through a semi-open roof. An air conditioning system controls the temperature and humidity on each stadium tier and on the football pitch. Air nozzles in the upper tiers exploit the buoyancy effect for the distribution of cool air, thereby saving energy. A steady-state, multi-region conjugate heat transfer model simulates the interaction between the building and environment using computational fluid dynamics. Six simulations are performed to investigate the thermal comfort in the stadium for different climatic conditions and duty cycles of the air conditioning system. All simulations measure the thermal sensation in the stadium's sectors based on the predicted mean vote and percentage of persons dissatisfied. They also assess the wet-bulb global temperature (WBGT) on the football pitch for the safety of the players, as required by FIFA guidelines. The results reveal that, for an external temperature of up to 48 °C and relative humidity of 70%, the air conditioning system guarantees a sensation of thermal neutrality, and the WBGT remains within the safety limit. When the cooling load is reduced by approximately 50%, most of the stadium's zones maintain thermal neutrality, and the risk of thermal stress to the players remains acceptable. Our research findings identify the conditions necessary to ensure a neutral thermal sensation in semi-open sport architectures, even in an extreme climate with high risk of thermal stress for the occupants.

1. Introduction

The climate conditions inside a football stadium affect the result of the match through the comfort levels of the occupants [1,2]. This concern becomes more serious for events experiencing extreme conditions, in which continuous thermal stress poses a significant risk to the health of the players and spectators [3,4]. The next FIFA World Cup is scheduled for 2022 and will be hosted in Qatar, where the summer air temperature and humidity can rise to 48ºC and 70%, respectively [5,6]. This event represents a challenging case study for defining new design guidelines that guarantee thermal comfort in hot and humid environments, as well as for optimizing the environmental sustainability of stadiums in such extreme climates (e.g., Ref. [7]).

A stadium is a semi-enclosed space [8], where human comfort depends on air temperature, humidity, solar radiation, and wind speed [9]. To understand how the thermal behavior of building typology affects these parameters, the designer must account for several complications that are characteristic of open and semi-open spaces:

- Outdoor and semi-outdoor spaces are exposed to highly transient environmental conditions, particularly solar radiation and wind speed [10];

* Corresponding author.
** Corresponding author.
E-mail addresses: g.losi001@unibs.it (G. Losi), a.bonzanini001@unibs.it (A. Bonzanini), andrea.aquino@unibs.it (A. Aquino), pietro.poesio@unibs.it (P. Poesio).

https://doi.org/10.1016/j.jobe.2020.101599
Received 28 December 2019; Received in revised form 18 June 2020; Accepted 19 June 2020
Available online 16 July 2020

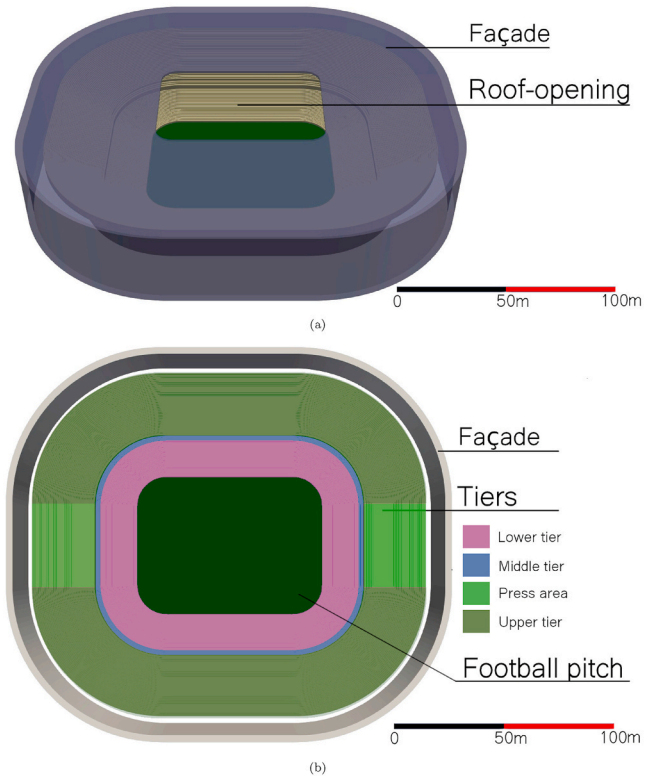

Fig. 1. Geometry of the stadium: (a) external view and (b) floor section. The different tiers and zones are colored as follows: the lower tier is violet, the middle tier is blue, the upper tier is green, and the press/media area is light green. (For interpretation of the references to color in this figure legend, the reader is referred to the Web version of this article.)

Table 1
Coefficients adopted in the Boussinesq model and in the vapor mass transport equation.

T_0	x_{v0}	β_T	β_{xv}	D_{xv}	Sc
300 K	0	$3.05 \cdot 10^{-3}\ K^{-1}$	0.61	$3.29 \cdot 10^{-5}\ m^2/s$	0.53

Table 2
Thermophysical and radiative properties of the solid domains.

Part	Material	$\kappa\ [W/(mK)]$	$c\ [J/(kgK)]$	$\rho\ [kg/m^3]$	α [−]	ε [−]
tiers	concrete	0.5	960	1500	0.6	0.95
pitch	grass, soil	0.13	1480	1800	0.8	0.9
façade	PTFE panels	0.3	950	$2.1 \cdot 10^{-3}$	0.35	0.8
ground	asphalt	0.75	920	2200	0.85	0.92

- The temperature distribution in large spaces is not uniform, and the uncertainty in measuring the comfort parameters interferes with their control [11];
- Human thermal sensation depends on the metabolic rate related to ongoing activities [12], which are different in each building space (e.g., the football pitch is characterized by a higher risk of thermal stress owing to the intensive activity of the players [13]);
- Each human body tends to continuously adapt itself to the climate via unique physical, physiological, and psychological mechanisms [14].

Due to these complex features, a methodology that guarantees an adequate comfort level for large and open spaces is still an area of open investigation [15].

Several authors have proposed new climate control methods based on a direct on-site measurement of the comfort parameters, which often require dedicated techniques to be applied in large open arenas and stadiums. Kang et al. [16] implemented a control scheme for the HVAC of an open-plan office. This system updates the room temperature target on the basis of the mean radiant temperature (MRT) and the predicted mean vote (PMV), which emulates how the human body adapts to environmental conditions. Zampetti et al. [17] pursued the same methodology, splitting a test room into subzones where a proportional integral derivative logic regulates the air conditioning based on the PMV measured in each subzone. Lee et al. [18] presented an infrared sampling method to simultaneously measure the MRT in multiple zones of a stadium using a single instrument, making the assessment of thermal comfort in large spaces more feasible (the high density of the occupants impedes the measurements). Fuertes et al. [19] presented an experimental and numerical analysis to study the effects of building material on the thermal comfort of the occupants. They classified the building materials using a thermal comfort parameter based on the transitory heat flow that occurs when the material comes into contact with the human body.

A different approach informs the design choices by a theoretical investigation of the influence of the architectural features (e.g., stadium shape, opening position, roof geometry) on the principal heat transfer parameters. Bouyer et al. [20] conducted a comprehensive morphological classification of stadiums around the globe (both ancient and modern) to investigate how the architectural parameters (e.g., façade porosity and roof opening angle) affect the climate within the stadium. They demonstrated the impact of the stadium shape (especially the roof) on the thermal comfort by mapping the Physiological Equivalent Temperature (PET) [21] on two models scaled for wind tunnels.

Szucs et al. [22] followed the same methodology to analyze how the environments of building sites affect the aerothermal comfort. They showed that the climate comfort in stadiums is mainly affected by the motion of air within the bowl (i.e., the volume confined by the spectator tiers and the roof). They also studied how the building geometry affects this airflow through a parametric analysis of a wind tunnel model.

Computational fluid dynamics (CFD) is a well-established technique for the theoretical investigation of thermal comfort as well as HVAC design and optimization. Focusing on large spaces, Nada et al. [23] presented a comprehensive CFD analysis of human thermal comfort in a theater. Their work related the main operative parameters of two different HVAC systems (one overhead and another under the floor) to the thermal comfort of the occupants by studying the effects of the airflow pattern, velocity, temperature, and the room architecture (theater height) on the PMV and percentage of persons dissatisfied (PPD) indices.

The number of studies that apply CFD to stadiums is increasing, but only a few of them have used simulations to assess human thermal comfort. There is a gap in the current literature on this topic, especially for stadiums located in hot and humid climates. Van Hooff et al. [24] used Lagrangian Particle Tracking to evaluate how different roof shapes protect the spectators against wind-driven rain. Uchida et al. [25] applied a custom CFD model to the Tokyo Olympic Stadium, but their analysis was limited to the effects of wind on the building structure. Other CFD assessments have focused on arenas designed for winter sports [26], which require careful design of the HVAC system to ensure an appropriate temperature for an ice rink or indoor swimming pool and an adequate thermal comfort level for the public [27]. Anastasios et al. [28] presented a CFD-guided comfort assessment of a stadium by calculating the air velocity and temperature within the Galatsi Arena (built in Athens for the 2004 Olympics) using the CFX software package [29] to map the PMV and PPD as comfort indices. However, this work examined a fully closed arena in a climate that is

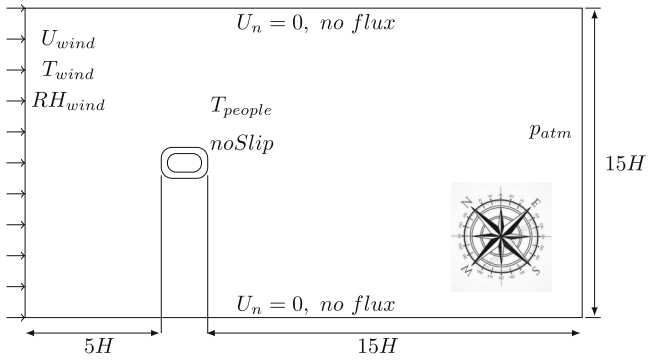

Fig. 2. Numerical domain and boundary conditions. The domain is oriented with its main axis along the NW – SE direction.

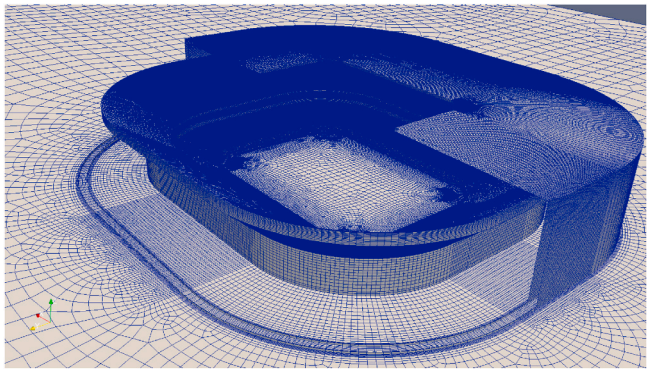

Fig. 3. A closer look at the mesh near the stadium. The external façade has been clipped to show the inner area.

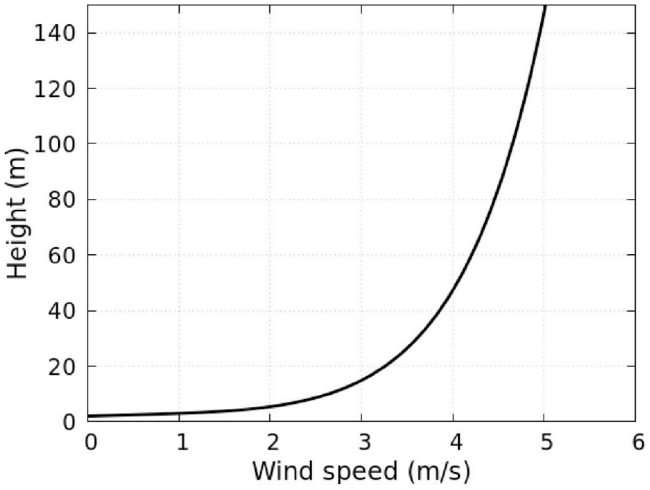

Fig. 4. Wind profile modeled following the ABL approach.

much less severe than that in Qatar. Ghani et al. [30] presented a case study of a football field in Khalifa (United Arab Emirates), which is a hot and humid environment. They analyzed the thermal behavior of the field experimentally and numerically, but they did not provide any results about the thermal comfort of the spectators and players.

This study simulates the thermal behavior of a stadium in Doha, Qatar, where the 2022 FIFA World Cup will be held. The aim is to develop a CFD model of the stadium that supports the HVAC design by evaluating the effects of the air conditioning operative parameters on the thermal comfort of the occupants. No similar approaches are available in the current literature, and the novelty of our case study is due to the extreme conditions (a hot and humid climate) that are studied, as well as the proposed methodology. Using CFD, we simulate the heat exchange that occurs through conduction, radiation, and convection between the stadium and the external environment. All simulations take into account several non-negligible environmental factors, such as wind speed, temperature, humidity, and solar radiation. They also account for the physical properties of the construction materials and the design variables of the HVAC system, such as the temperature and flow rate of the cooling air.

1.1. Case study

Our case study is characterized by distinctive features typical of a football stadium for international competitions [31]. Thus, the theoretical predictions used for design purposes are suitable for comparisons with experimental data. The stadium (Fig. 1) is in an oval shape and allows a total capacity of 47,000 seated spectators. The bleachers running along the internal perimeter are divided into three different levels:

1. The lower tier (colored in violet), from pitch level to 10.6 m high, can host 20,000 spectators;
2. The middle tier (colored in blue), from 13.75 m to 15 m high, can host 1000 spectators;
3. The upper tier, from 19 m to 39 m high, can host 26,000 spectators and is divided into two areas, the public bleachers (25, 000 spectators, colored in green) and the press/media area (1000 spectators, colored in light green).

The total internal volume of the stadium is about $1.5{\cdot}10^6$ m^3, and it is confined by an external shell that forms the open roof and the façade. The latter could be a thin wire grid, a fabric mounted on metal supports, or a more complex paneled structure. Details of the materials used for this analysis are provided in Section 3.1. The entrance doors are moving panels of the external façade. However, we do not include them in the geometrical domain because in all simulations, the match is ongoing, and the entrance doors are closed. The roof opening is the only possible entrance for the wind and solar radiation that contribute to the properties of the air within the stadium.

The exterior stadium dimensions are 272 m × 250 m x 47 m. The stadium is situated in Doha, Qatar, where the 2022 FIFA World Cup will be held between November 21 and December 18. During winter, the mean humidity of Doha varies between 60-70%, and the temperature varies between 32 °C and about 40 °C (the highest recorded observation [32]). Such conditions expose the occupants to high risk of thermal stress; therefore, an HVAC system controls the climate on the tiers and the football pitch to guarantee adequate thermal comfort in the stadium. Cooling air nozzles are installed in the upper tier to cool down the middle and lower tiers through the buoyancy effect; the cooler air moves downward and displaces the lighter layers of hot air, thereby establishing an internal recirculation. The chilled air is supplied inside the stadium at a temperature between 19-23 °C after being moisturized with a relative humidity of $RH = 50\%$.

2. Material and methods

2.1. Physics equations

Both the inside and outside of the stadium are described using a steady-state, multi-region conjugate heat transfer solver available in the OpenFOAM software package and modified to account for vapor fraction transport, buoyancy effects, and solar radiation. We simulate the heat transfer due to conduction, convection, and radiation; therefore, the computational domain should account for both the solid and fluid regions of the stadium and the air it contains. The chtMultiRegionSimpleFoam OpenFOAM solver is adopted as a starting point. It is

Table 3
Cooling nozzle air properties: volumetric flow rate, DBT, and relative humidity.

Simulation	Wind conditions		HVAC settings		
	T [°C]	RH [%]	T [°C]	RH [%]	Flow rate [m^3/s]
SIM01	30	70	19	50	108
SIM02	35	70	19	50	108
SIM03	40	60	19	50	108
SIM04	35	70	21	50	54
SIM05	35	70	23	50	54
SIM06	48	60	19	50	108

Table 4
Acceptable range for the use of PMV/PPD indices [46,47].

Environmental parameter	Unit	Acceptable range
Air temperature	°C	10–30
Mean radiant temperature	°C	10–40
Relative air velocity	m/s	0–1
Partial pressure of water	Pa	0–2700
Individual parameter	**Unit**	**Acceptable range**
Metabolic rate	MET (1 MET = 58.2 W/m^2)	0.8–4
Thermal resistance of clothing	CLO (1 CLO = 0.55 m^{2}K/W)	0–2

a steady-state solver for buoyant, turbulent fluid flow and solid heat conduction with conjugate heat transfer between solid and fluid regions, with the option to model radiation.

In the solid regions (the ground, the tiers, the façade, and the pitch), heat transfer is simulated by solving

$$\frac{\partial T_s}{\partial t} = D_T \nabla^2 T_s + S_T, \tag{1}$$

where T_s is the temperature in the solid domain, D_T is the thermal diffusivity, and S_T is a thermal source term.

In the fluid region of the air, the energy equation is solved for the enthalpy h with

$$\frac{\partial \rho h}{\partial t} + \mathbf{u}\cdot\nabla(\rho h) + \rho\mathbf{u}\cdot\nabla\left(\frac{1}{2}\mathbf{u}\cdot\mathbf{u}\right) = -\nabla\cdot\mathbf{q} + S_H, \tag{2}$$

where ρ represents the fluid density, **u** is its velocity, **q** is the thermal flux, and S_H is a source term, which is used to include the solar radiation in the equation. The specific heat c_p is assumed to be constant because the temperature range analyzed is small. At the interface between the solid and fluid regions, the heat balance is modeled through coupled boundary conditions. That is, equal temperatures are imposed on the coupled patches.

The mass and momentum conservation equation, solved in the fluid region, are

$$\frac{\partial \rho}{\partial t} + \nabla\cdot(\rho\mathbf{u}) = 0, \tag{3}$$

$$\frac{\partial \mathrm{u}}{\partial t} + \mathbf{u}\cdot\nabla\mathbf{u} = -\frac{1}{\rho}\nabla p + \nu\nabla^2\mathbf{u} + \rho'\mathrm{g}, \tag{4}$$

where **u** is the air velocity, p is the pressure, ν is the kinematic viscosity, g is the acceleration due to gravity, and ρ' is the density variation due to the differences in temperature and vapor mass concentration. The fluid phase is considered compressible. Furthermore, the buoyancy forces are considered by adopting the Boussinesq approximation (as described in 33), which is

$$\rho' = -\beta_T(T - T_0) - \beta_{xv}(x_v - x_{v0}), \tag{5}$$

where T is the fluid temperature; $x_v = \frac{m_a}{(m_v+m_a)}$ is the vapor mass concentration (m_a and m_v are the mass of air and of vapor, respectively); T_0 and x_{v0} are the temperature and vapor concentration references, respectively; and β_T and β_{xv} are the thermal expansion and vapor expansion coefficients, respectively. The values of these coefficients are reported in Table 1, and they were originally found in Ref. [33].

The vapor concentration transport equation is not implemented in the original solver available in OpenFOAM. Therefore, its solution has been added to the solving algorithm.

Moreover, in OpenFOAM, only the buoyancy effects given by temperature are present. Hence, a source term (eq. (5)) has been added in the momentum balance equation (eq. (4)) to account for the contribution of the vapor concentration. The latter is transported in the fluid phase according to

$$\frac{\partial x_v}{\partial t} + \mathbf{u}\cdot\nabla x_v = \nabla^2\left(\left(D_{xv} + \frac{\nu_t}{Sc}\right)x_v\right), \tag{6}$$

where D_{xv} is the vapor diffusion coefficient and Sc is the Schmidt number, both of which are reported in Table 1. The k-ω SST turbulence model is now solved. The turbulent specific dissipation rate (ω) is

$$\frac{D}{Dt}(\rho\omega) = \nabla\cdot\left(\rho D_\omega\nabla\omega\right) + \frac{\rho\gamma G}{\nu} - \frac{2}{3}\rho\gamma\omega(\nabla\cdot\mathbf{u}) - \rho\beta\omega^2 - \rho\left(F_1 - 1\right)CD_{k\omega} + S_\omega, \tag{7}$$

and the turbulent kinetic energy equation is

$$\frac{D}{Dt}(\rho k) = \nabla\cdot\left(\rho D_k\nabla k\right) + \rho G - \frac{2}{3}\rho k(\nabla\cdot\mathbf{u}) - \rho\beta^*\omega k + S_k. \tag{8}$$

The wall function adopted in this work is derived from Ref. [34] and allows the modeling of the Atmospheric Boundary Layer (ABL) in each domain. In the original work of [34], the wall functions for the turbulent kinetic energy (k) and the dissipation rate (ε) are available, along with the one for wind velocity. As the $k-\omega$ SST turbulence model is selected as the most suitable for the stability of our simulation, we derived the wall function for the missing specific dissipation (ω) to have a complete description of the flow.

Solar radiation is incorporated via the radiation model solarLoad available in the OpenFOAM package. The solar fluxes are computed following the Fair Weather Conditions Method from the ASHRAE Handbook [35]. The primary solar heat fluxes, their reflective fluxes on walls, and the diffusive sky radiative fluxes are also included. The location of Doha is described by its local standard time meridian, longitude, and latitude. As the FIFA World Cup will be played in winter, December 15 and 4 p.m. are taken as a reasonable date and time, respectively, for a possible match, and this is inserted into the specifications required to compute the solar radiation fluxes. The air scatter phenomenon is also taken into account and modeled as isotropic.

The thermophysical properties (thermal conductivity κ, specific heat c, and density ρ) and radiative properties (emissivity ε and absorptivity α) of the solid domains (pitch, tiers, façade, and ground) are reported in Table 2. The thermal diffusivity D_T, used in Eq. (1), is computed from the thermal conductivity, the specific heat, and the density as $D_T = k/(c\rho)$. The thermophysical properties of air, namely the dynamic viscosity and specific heat at constant pressure, are $\mu = 1.8\cdot10^{-5}\ kg/(ms)$ and $c_p = 1000.5\ J/(kgK)$, respectively.

The presented model solves the differential equations by applying the finite volume method. It uses the Semi-Implicit Method for Pressure Linked Equations (SIMPLE) as the resolution algorithm and the Gaussian integration as the discretization scheme. The interpolation scheme is linear. We check the accuracy of the solutions based on the residuals of the following variables: pressure, velocity components,

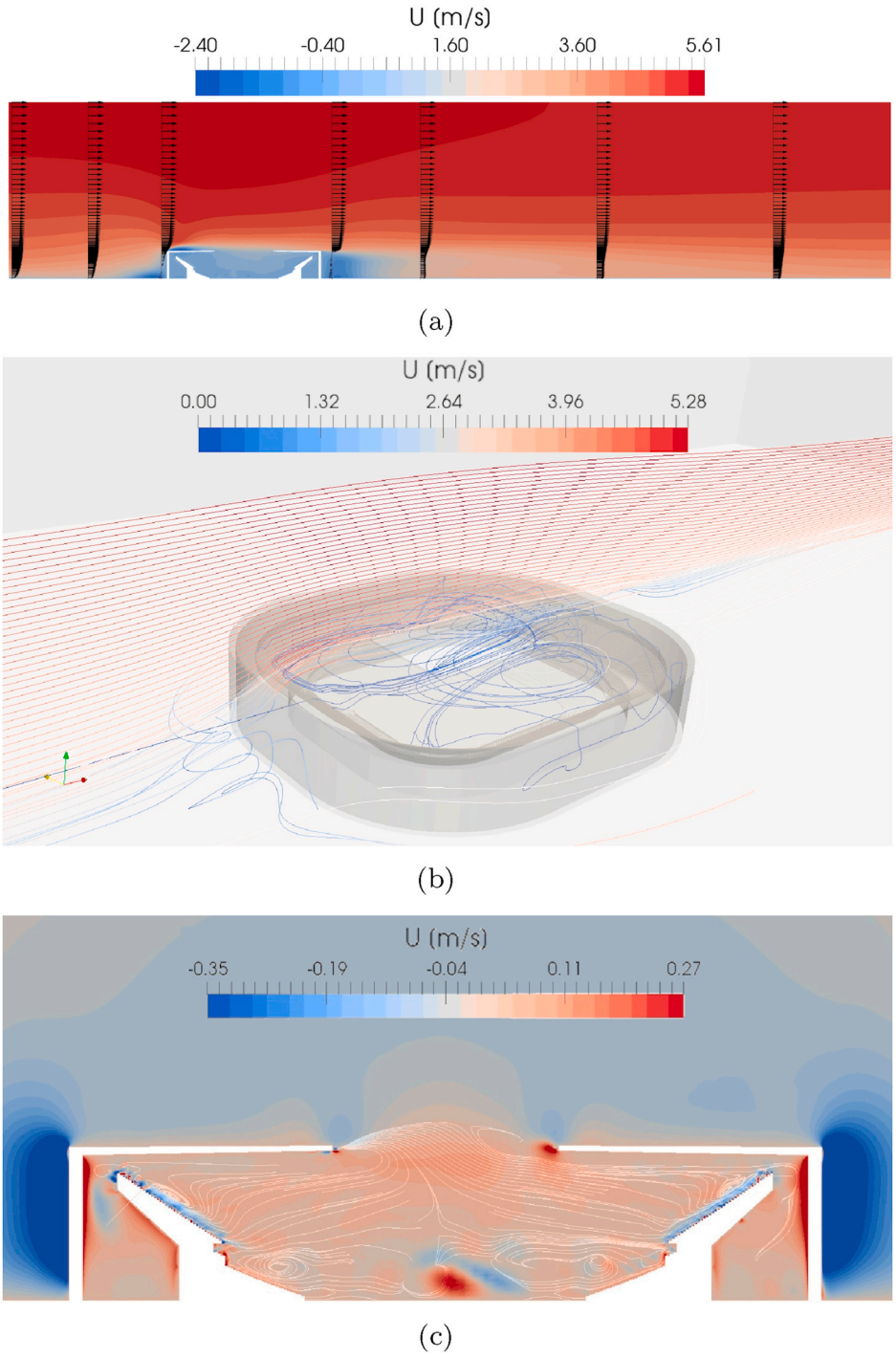

Fig. 5. Simulation of the air velocity field: (a) the wind impacts the building (streamwise component of the wind velocity field); (b) the air penetrates from the roof and affects the circulation inside the stadium; (c) the HVAC distributes cool air from the upper tiers to the football pitch.

Table 5
Risk of heat illness related to the WBGT index.

WBGT [$^{\circ}C$]	Risk of thermal injury
24.0–29.3	Moderate
29.4–32.1	High
≥ 32.2	Extreme

enthalpy, and the k-ω turbulence parameters. In detail, all solutions converge after more than 45,000 iterations, when the residuals are stable and below the limits of 4×10^{-4} (velocity components), 0.12 (pressure), 4×10^{-3} (enthalpy), 5×10^{-6} (k), and 4×10^{-5} (omega). Owing to the lack of experimental results, we cannot validate the predictions of our model. Either the limited analyses of the indoor climate in stadia that are available in literature do not relate to the thermal comfort of the occupant or they refer to different architectures and climates than those considered in our case study. However, this OpenFOAM solver was successfully used for the thermal comfort assessments of existing buildings (e.g., the semi-Olympic pool at Bish-

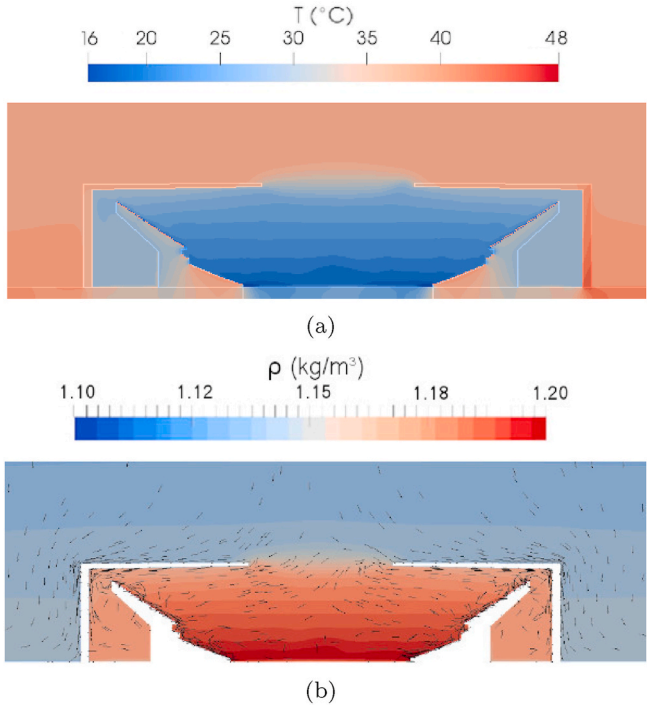

Fig. 6. Cross section of the stadium (sun exposed side on the right): (a) temperature distribution; (b) air stratification generated by buoyancy.

op's University [27], SC Johnson's Fortaleza Hall [36], and a classroom in the University College Cork [37]).

2.2. Numerical domain and boundary conditions

According to the classification given by Ref. [38], this study falls into the category of micro-scale urban aerodynamics, as the maximum horizontal length scale ranges between 1 and 10 km. The external domain (Fig. 2) representing the bounding box outside the stadium structure is designed according to the guidelines given in Refs. [39]. This means that only one building is modeled. Thus, the characteristic length scale is the height H of the stadium, and all the dimensions of the bounding box are scaled accordingly. The vertical extension of the domain is $5H$, and the width is $15H$, leading to a blockage factor of 3%. The approach flow region (i.e., in front of the stadium) is also $5H$, and the wake region (i.e., behind the stadium) is $15H$ to allow the flow to re-establish itself after it passes over the obstacle. The dimensions of the whole domain are $1272m \times 750m \times 250m$ (length × width × height).

In order to coherently simulate the flow outside and inside the stadium as well as the effect of wind on the large aperture of the roof, the mass and energy exchanges between the external and internal spaces are simultaneously solved (i.e., using the coupled approach), making the "sealed body assumption" no longer valid. Owing to the roof's aperture, the kinetic energy of the approaching wind is not dissipated, as pointed out in Ref. [40]. Similarly [41], found a strong interaction between the interior and the exterior domains. The main challenge of this methodology is the requirement to account for all length scales of the domain, ranging from 0.5 m (i.e., the height of the bleachers) to approximately 1 km (the length of the outer domain). In this situation, producing a high-quality, high-resolution, and computationally efficient grid is very demanding, but it is necessary to obtain accurate results. The meshing technique developed by Ref. [42] has been applied, producing a hybrid, structured-unstructured grid that ensures a high-quality refinement in the façade region. The grid also allows a high resolution for the boundary layer, as it conforms to the complex geometry of the bleachers and gradually becomes coarser in the far field (Fig. 3). The elements are all hexahedral, and the total number of cells is approximately 11×10^6. If only the fluid domain is considered, the number of cells is approximately 6×10^6.

In the simulated domain, two different regions are distinguished: the central region, where the buildings and other possible obstacles to the wind are modeled explicitly, and the upstream and downstream zones (previously introduced as approach flow region and wake region, respectively), where the obstacles are not modeled explicitly but through their effect on the flow [43]. This work explicitly simulates the stadium only, and no obstacles or other buildings are placed directly in the domain. However, the roughness due to small-scale objects and small buildings is taken into account implicitly by adopting wall functions for the ABL. At the inlet, the wind velocity profile is set following the specifications for an urban environment. The mean wind velocity at the building site is about 3.7 m/s [32], and the reference wind velocity is 2.1 m/s at the reference height of 5 m. The resulting velocity profile is shown in Fig. 4.

Meteorological data [44] show that in December, the wind blows mainly from the northwest in Doha. This fact has been modeled by varying the angle between the velocity components at the inlet and the solar position. The relative humidity of the air at this time of the year ranges from 60% to 70%. Thus, these two values were defined at the inlet boundary as transported by the wind. The mean maximum temperatures in Doha in December from 1996 to 2013 ranged from $25°C$ to $30°C$. However, considering recent studies that found warming trends in the region [45], we decided to consider higher temperatures as well. Hence, the Dry Bulb Temperature (DBT), adopted as the inlet wind temperature, was assigned the values of $30°C$, $35°C$, $40°C$, and $48°C$.

The boundary condition used for the air conditioning system is a volumetric flow rate applied to selected surfaces corresponding to the vertical walls of the upper-tier bleachers and the surface encompassing the pitch. The air flowing from the nozzles has a DBT of $19°C$, $21°C$, $23°C$ and has a relative humidity of 50%. Finally, the presence of the spectators in the stadium is accounted for by setting a fixed temperature ($37°C$) on the seats following the methodology adopted by Van Hooff and Blocken (2010). The combination of the

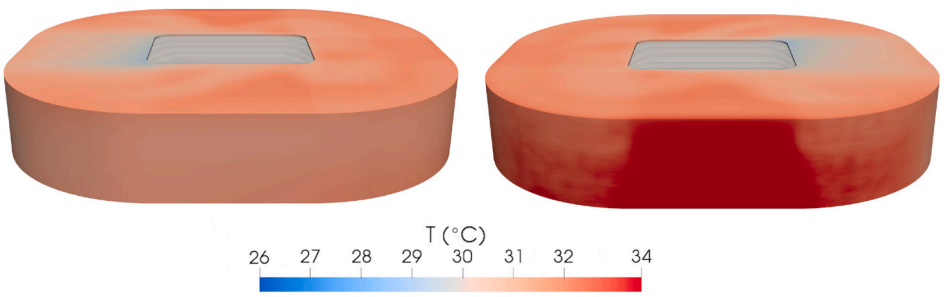

Fig. 7. Heating of the stadium's façade by solar radiation: shaded side (left); sun exposed side (right).

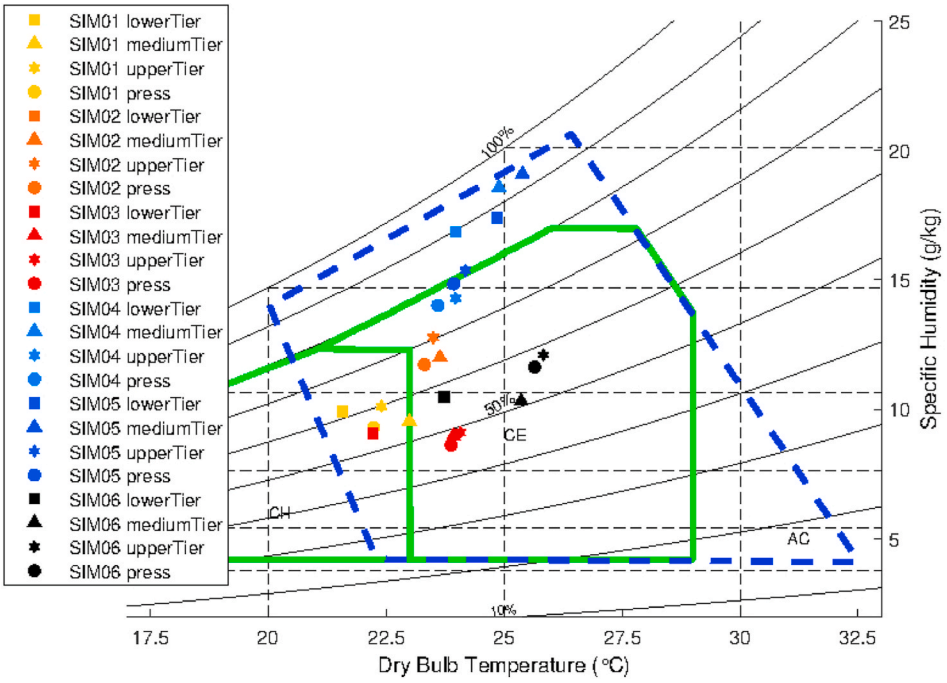

Fig. 8. Results of the simulations, shown through the Givoni diagram, along with the winter comfort zone (CH), the summer comfort zone (CE), and the ventilated comfort zone (blue line). (For interpretation of the references to color in this figure legend, the reader is referred to the Web version of this article.)

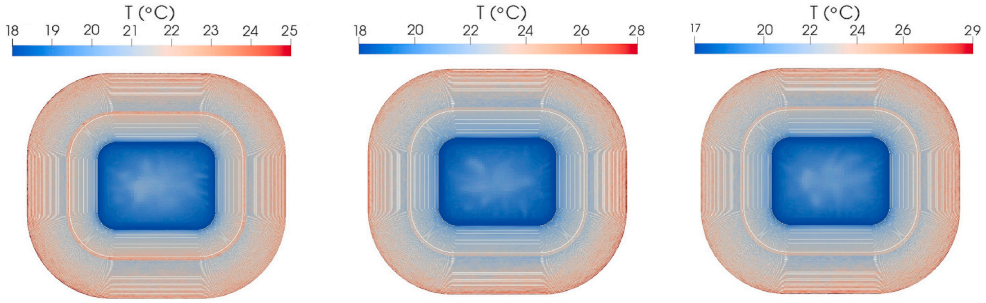

Fig. 9. Temperature field sampled at a distance of 0.5 m from the surface of the tiers and the pitch: SIM01 (left); SIM02 (middle); SIM03 (right).

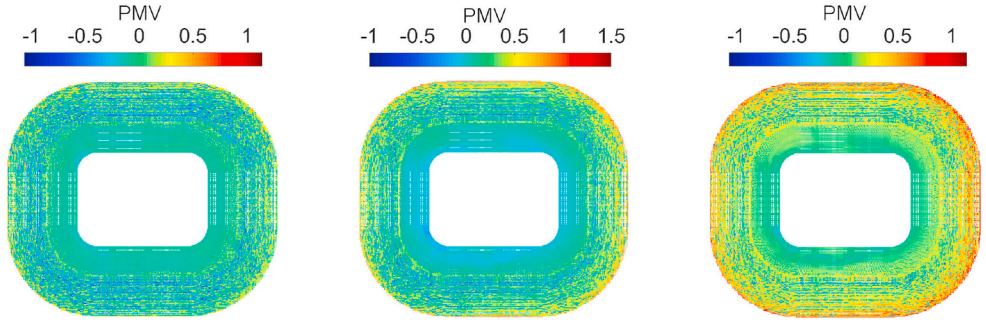

Fig. 10. Visible range of the PMV values on the tiers: SIM01 (left); SIM02 (middle); SIM03 (right).

wind characteristics and the cooling system conditions are reported in Section 3.3.

2.3. Operating conditions and simulation steps

Six different combinations of wind and cooling conditions are simulated (Table 3). The wind temperature has the values of 30°C, 35°C, 40°C, and 48°C, and its relative humidity has the values of 60% and 70%. The values of the cooling temperature of the air from the cooling system located on the pitch level are 19°C, 21°C, and 23°C, whereas those of the flow rate are 54 m^3/s and 108 m^3/s; the relative humidity is kept constant at 50%. The cooling systems located on the upper tier and press/media area are set to cooling temperature of 19°C and flow rates of 225 m^3/s and 20 m^3/s, respectively. These values are kept constant in all five simulations. The adopted volumetric flow rate estimations are based on the tier capacity and the required cooling of the pitch. In all simulations, the occupancy of the stadium is at full capacity, and we omit the building operation schedule because it is not necessary to consider it in our steady-state analysis.

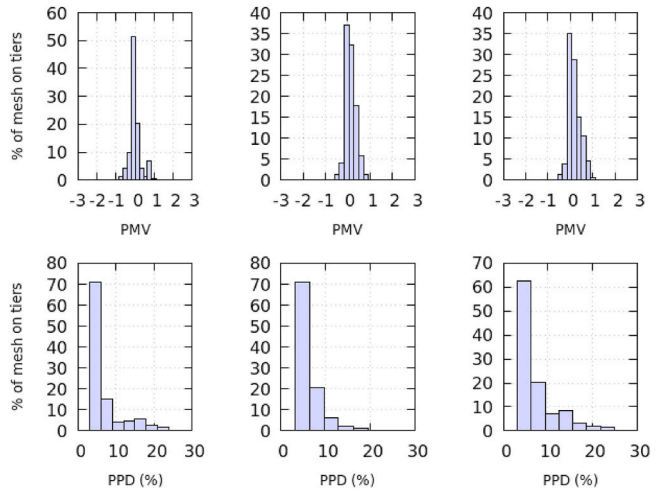

Fig. 11. Histograms of the PMV and PPD indices for SIM01, SIM02, and SIM03 (left to right).

2.4. Thermal comfort indicators

The analysis of thermal comfort is limited to the stadium's bowl, i.e., the space enveloped by the tiers, football pitch, and open roof; this is a semi-outdoor space, where the climate is controlled by mechanical ventilation (i.e., centralized HVAC system). We use the PMV and PPD indices, defined in the ISO Standard 7730 [46], to analyze the thermal comfort at the tiers (i.e., the thermal sensation of the spectators). The PMV is the mean value of the ratings given by a sufficiently large sample of people for a range of thermal sensations. The range spans from -3 to +3, where neutral is represented by zero, very cold is represented by -3, and very warm is represented by +3. Once the PMV is known, the PPD is calculated to determine the percentage of dissatisfied people (i.e., people that vote a thermal sensation greater than or equal to 2 or less than or equal to -2).

The PMV and PPD indices depend on six parameters: the metabolic rate, thermal resistance of clothing, air temperature, MRT, relative air velocity, and relative humidity. These indices are applicable only in moderate environments [46,47], where the parameters mentioned above fall within the ranges reported in Table 4.

As individual-level parameters, we assume a clothing value of 1.0 CLO and metabolic rate of 1.2 MET. The MRT is equal to the mean temperature of the stadium's zone under analysis [48]. The other environmental parameters are sampled from the CFD results at a distance of 0.5 m from the surface of the tiers; these results show that the environmental parameters in our case study are within the ranges recommended in the technical regulation (see the air temperature, velocity, and humidity in Figs. 5c, 8 and 9, 13); therefore, the assessment of the thermal comfort at the tiers based on the PMV and PPD indices is justified.

An alternative methodology for the analysis of thermal comfort is adaptive theory [49]; this method links the expressed thermal sensation to the response of the occupants (i.e., how they adapt to the climatic conditions by interacting with the environment). The adaptive theory depends on the variables that influence the individual response [50–52]: the effects of the outdoor temperature on the indoor climate, the building use, access of the occupants to the ventilation system settings, and time-scale at which the individual response occurs. We cannot apply the adaptive theory to our research because the current standards [53–59] are applicable only in naturally ventilated environments or when the HVAC is disabled. The comfort assessment in this work focuses on a semi-closed environment, i.e., the stadium's bowl, which is controlled by centralized mechanical ventilation. The HVAC decouples the indoor climate from the external environment (results will show that the open roof contributes only to the natural illumination of the space), and the occupants cannot adjust the ventilation settings. Furthermore, we use a CFD steady-state model that cannot simulate any variations in the climate and occupant's response over time.

To evaluate the thermal conditions on the pitch, we use the wet-bulb globe temperature (WBGT) index, which is used in industry, the army, and sports to evaluate the heat stress level of physical activity [60]. FIFA has declared guidelines for the medical teams, reported in Ref. [61] and briefly presented in Table 5, indicating the risk of thermal injury as function of the WBGT.

This index takes into account the effect of the air temperature, solar radiation, humidity, and wind speed. It is computed via a linear combination of the wet-bulb temperature T_{wb}, the globe temperature T_g, and the dry-bulb temperature T_{db}:

$$WBGT = 0.7T_{wb} + 0.2T_g + 0.1T_{db}. \quad (9)$$

To compute the WBGT on the pitch, the results of the numerical simulations are sampled at 0.5 m above its surface. The wet-bulb temperature is computed using the relation proposed by Ref. [62], while the globe temperature is estimated by employing the relation of [63].

3. Results and discussion

In this section, the interaction between the stadium and the environment are shown based on the results of SIM02. The analysis of the thermal comfort of the spectators and players, and the temperature distribution on the pitch are described in the following paragraphs. First, the wind conditions are varied, and the cooling settings are held constant (comparison of SIM01, SIM02, and SIM03). Then, the cooling conditions imposed on the pitch are varied while the wind characteristics are kept constant (comparison of SIM02, SIM04, and SIM05). Finally, the results for the extreme climate conditions in SIM06 are presented.

3.1. Stadium and its environment

This section illustrates the effects of the environment on the stadium's bowl based on qualitative results that are available in all simulation cases, such as the velocity field inside and outside the bowl, effect of radiation on the tiers and the ground, and air density distribution. As shown in Fig. 5a, the ABL breaks before the stadium and reattaches before the end of the domain. When the wind encounters the

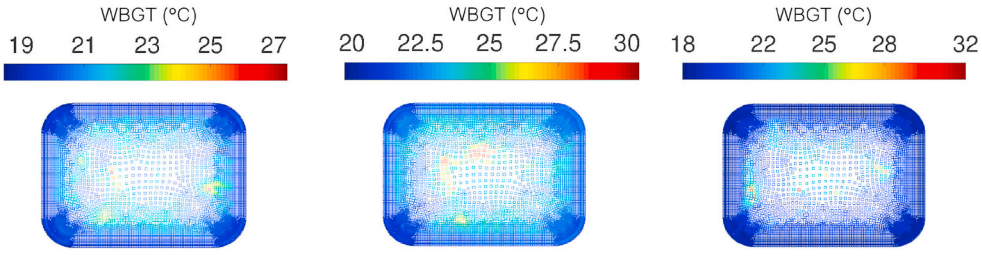

Fig. 12. WBGT values on the football pitch: SIM01 (left); SIM02 (middle); SIM03 (right).

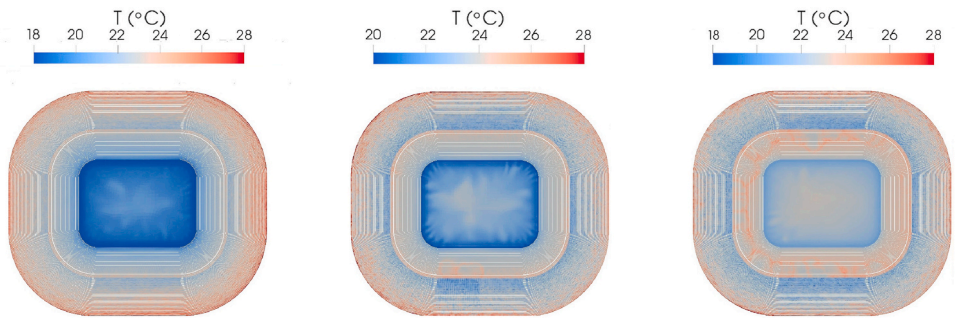

Fig. 13. Temperature field sampled at a distance of 0.5 m from the surface of the tiers and the pitch: SIM02 (left); SIM04 (middle); SIM05 (right).

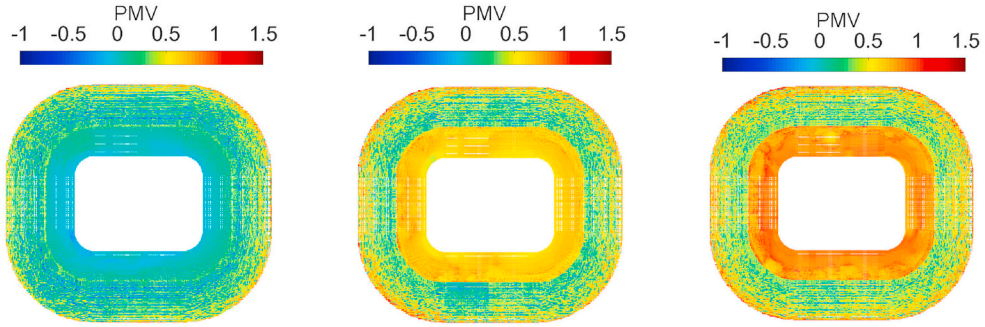

Fig. 14. Visible range of the PMV values at the tiers: SIM02 (left); SIM04 (middle); SIM05 (right).

upper windward corner of the façade, a thin backflow is generated along the external surface of the roof. The air accelerates and changes its direction to penetrate into the stadium bowl from the opening on the roof. The streamlines in Fig. 5b show that the wind actively contributes to the air distribution inside the stadium. The airflow separates into two horizontal vortices centered on the wind-oriented axis. It circulates around the stadium perimeter, reaching all tier levels and the entire football field. Finally, the cross section in Fig. 5c shows the cold air flowing down from the upper tier to the lower tier, and then the warm air and cold air are mixed at the center of the pitch.

The temperature distribution in the entire domain is shown in Fig. 6a. The average temperature of the ground is 45°*C*, which is consistent with the temperature in Qatar during the late autumn season. The parts of the ground directly exposed to the solar radiation (right side) are at a higher temperature than the shaded sides. Air stratification occurs inside the stadium via the buoyancy mechanism; this effect actively contributes to a homogeneous distribution of the cooling air, from the upper levels of the tiers down to the football pitch (see Fig. 6b, where the vectors represent the vertical component of the velocity superimposed on the density field). The air temperature gradually increases from the coldest value on the football pitch, thus reducing the risk of thermal injuries. In the indoor spaces below the tiers, the air movement is limited to a thin layer on the interior of the external façade and no temperature stratification occurs. Hence, the partitioning of these zones into subzones (e.g., as stores and offices) is irrelevant for the air distribution inside the stadium bowl.

The combined effects of the wind and solar radiation are shown in Fig. 7. The solar radiation increases the temperature on the façade exposed to the southwest (i.e., it is directly exposed to the solar radiation), and the upwind part of the roof is cooled by the wind. The sunlight penetrates inside the stadium from the open roof, contributing to the natural lighting of the stadium bowl; however, the air conditioning system maintains the irradiated area at a similar temperature to that of the areas not directly exposed to the sun (see the temperature at the tiers in Figs. 9 and 13).

3.2. Comfort assessment at the tiers

The Givoni diagram [64] evaluates the comfort in each specific region of the tiers (i.e., the lower tier, middle tier, upper tier, and press seats). Before comparing the results of the PMV and PPD, the thermal comfort for all five simulations are compared using the Givoni diagram (Fig. 8). The areas inside the green and blue lines represent, respectively, the winter comfort area (CH), the summer comfort area (CE), and the comfort area in the case of ventilation (AC). The points represent the mean values of the temperature and specific humidity for each of the tier sections. The middle tier, the upper tier, and the press seats of SIM02 and SIM03 are inside the summer comfort zone, which also occurs for the upper tier and the press seats of SIM04 and SIM05. In contrast, all the zones of SIM01 and the lower tiers of SIM02 and SIM03 are in the winter comfort zone. This indicates that these zones are comfortable, but their temperature and specific humidity could be increased, thereby reducing the cooling costs by using a higher nozzle temperature. The middle tiers and lower tiers of SIM04 and SIM05 are outside the summer comfort zone, but inside the ventilated comfort zone. However, the condition of the middle tier is borderline, and it can be improved. In the case of extreme conditions (SIM06), all the tiers fall inside the summer comfort zone, which demonstrates that the HVAC system can provide a comfortable environment in harsh conditions.

3.2.1. Comfort assessment for varying wind conditions: SIM01, SIM02, and SIM03

The temperature distributions on the pitch and at the tiers are shown in Fig. 9. The temperature field is sampled at 0.5 m above the pitch and above the three tiers of bleachers. A comparison is made between the three tested wind temperatures, and the air conditioning system provides the desired temperatures. Even with an outside temperature of 40°*C* (SIM03), the temperature range inside the building is kept below 30°*C*.

The chosen settings for the air conditioning system provide a comfortable environment at all tiers of the bleachers. The results in Fig. 10 show that thermal neutrality occurs everywhere at the tiers. For

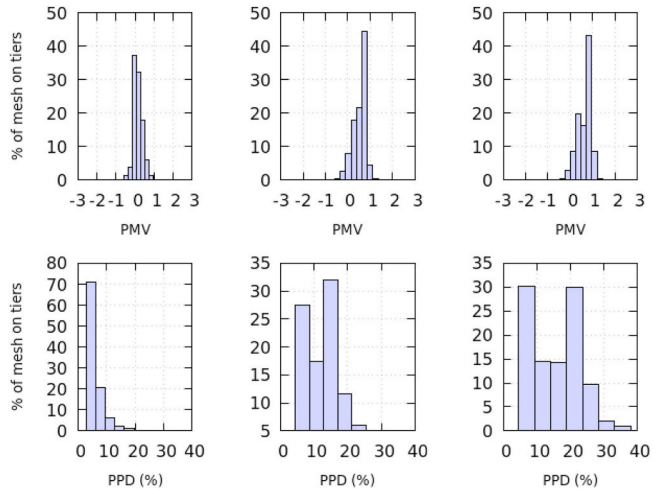

Fig. 15. Histograms of the PMV and PPD indices in SIM02 (left column), SIM04 (center column), and SIM05 (right column).

any given wind condition, the resulting PMV is in the range of -0.2 – 0.2. This result is consistent with the standards that recommend a PMV value of approximately zero and deviation of ± 0.5 [65]. In SIM02 and SIM03, a PMV of roughly one is observed on the higher seats of the upper tier, because the cold air from the nozzles is focused on the lower levels of the stadium. Moreover, the comfort level is lower on the right side of the upper tier because of the wind entering the building. The histograms in Fig. 11 present the distributions of PMV and PPD over the tiers, weighted on the mesh of the entire stadium. In all tested cases, the most frequently observed values of the PMV and PPD are approximately zero and 5%, respectively; thus, the HVAC successfully guarantees a neutral thermal condition in the entire stadium bowl.

Finally, the results in Fig. 12 indicate that the WBGT is far below the maximum prescribed temperature of 32°C in all three simulations, except for some spots in SIM03. However, for most of the pitch of the latter, the index is lower than 24°C, indicating a low risk of thermal injury.

Given the results presented in this section and the conditions proposed in SIM01, SIM02, and SIM03, it is possible to guarantee that a comfortable environment exists on almost all the tiers and that the players are not exposed to the risk of thermal injuries. However, the mean DBT registered on the pitch ($\approx 19.5°C$) is low if it is compared to the wind temperature, and achieving this condition may be expensive. Thus, in the next section, three additional simulations are compared for the following scenario: the temperature of the air flowing from the cooling nozzle located on the pitch is increased, but the wind temperature is kept constant.

3.2.2. Comfort assessment for varying cooling conditions on the pitch: SIM02, SIM04, and SIM05

Results in Fig. 13 show the temperature, sampled at 0.5 m above the surface, throughout the stadium. As the cooling temperature of the pitch nozzles is increased and the volumetric flow rate is reduced, the temperature rises on the field and on the lower tier, as expected. However, in the whole stadium, the temperature is kept below 30°C.

The PMV distributions in the three simulations are shown in Fig. 14. With respect to SIM02, the PMV increases in the lower and upper tiers as the cooling temperature of the pitch nozzle increases. This indicates that the thermal sensation of the spectators at this level moves from neutral (in SIM02, PMV ≈0) to slightly warm (PMV ≈0.6 and 0.9 in SIM04 and SIM05, respectively). Hence, the cooling of the lower tier is also influenced by the pitch cooling conditions and does not rely only on the cooling provided for the upper tiers.

The histograms of the PMV index in Fig. 15 (top) show that the most frequent PMV shifts from ≈0 to ≈0.8, which is consistent with the changes in the cooling temperature of the pitch nozzles. Moreover, the trend is visible also for the PPD index in Fig. 15 (bottom). The distribution maximum is around 5% in SIM02, whereas at higher cooling temperatures, more spectators appear to be dissatisfied with the thermal conditions. However, this percentage of dissatisfied persons is acceptable, considering the cost reduction achieved by increasing the nozzle temperature and by reducing the flow rate. In a future study, these two parameters can be further tuned to minimize the cost and maximize thermal comfort.

The distribution of the WBGT index on the pitch is reported in Fig. 16. As expected, this index rises as the air temperature of the nozzles increases. A moderate risk of thermal injury is expected in the case of SIM04 and SIM05, and, in particular, on the right side of the pitch in SIM05. The latter is due to the wind, which enters the stadium and carries warm and humid air. In this case, the humidity of the wind affects more than the temperature in the WBGT index. Accurate tuning of the temperature, volumetric flow rate, and humidity of the air flowing from the pitch nozzles should be carried out in a future study as well.

3.2.3. Comfort assessment for extreme conditions: SIM06

The evaluation of the thermal comfort under extreme conditions (SIM06) is reported in Fig. 17, which shows the PMV and PPD indices at the tiers. The PMV varies between 0.4 – 1 in all the bleachers, except for the highest zone of the upper tier, where the index rises to 2. This indicates that the spectators feel a slightly warm sensation in the whole stadium except for the upper part, where the spectators report being uncomfortable. A possible explanation of this result is that the cold air supplied by the HVAC system descends as the hot air enters through the open roof. Hence, a dedicated cooling apparatus to supply cold air to the higher bleachers could be necessary for these extreme conditions. The resulting WBGT distribution on the field (Fig. 17) shows that safe thermal conditions are ensured for the players even under these extreme conditions, which is a result of the dedicated HVAC system located around the pitch.

The histograms of the PMV and PPD indices (Fig. 18) show that most of the spectators are satisfied with the thermal conditions. However, the right-hand tails of the distributions reach high values, which represent the dissatisfied persons in the higher zones of the stadium.

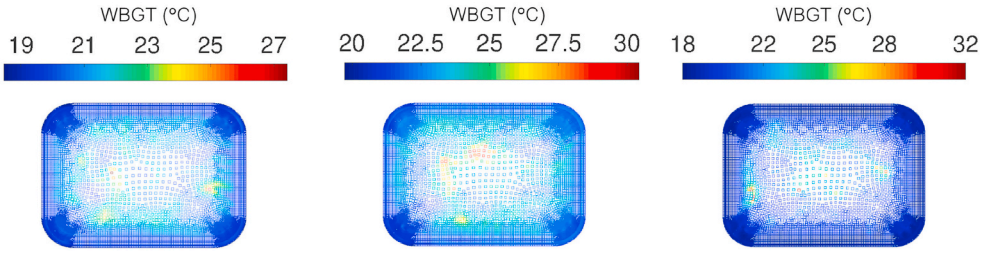

Fig. 16. WBGT values on the football pitch: SIM01 (left); SIM02 (middle); SIM03 (right).

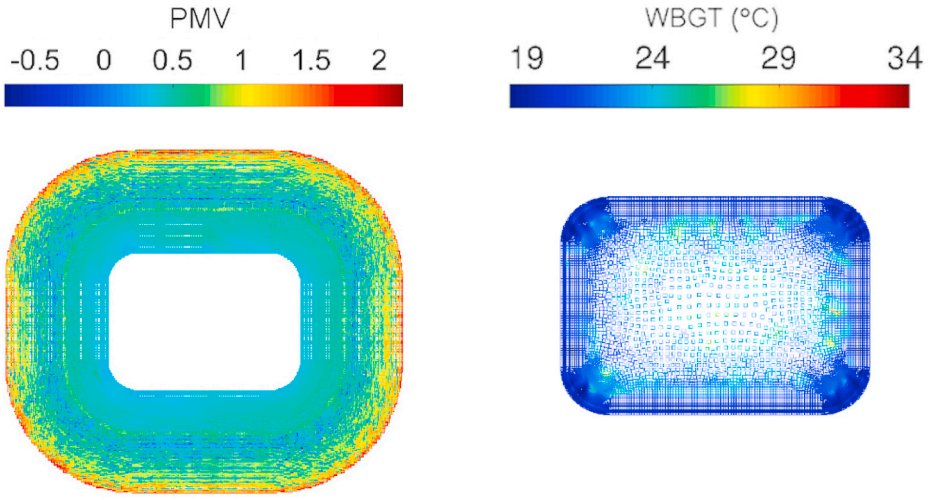

Fig. 17. The visible range of the PMV on the tiers (left) and the WGBT on the football pitch (right) in SIM06.

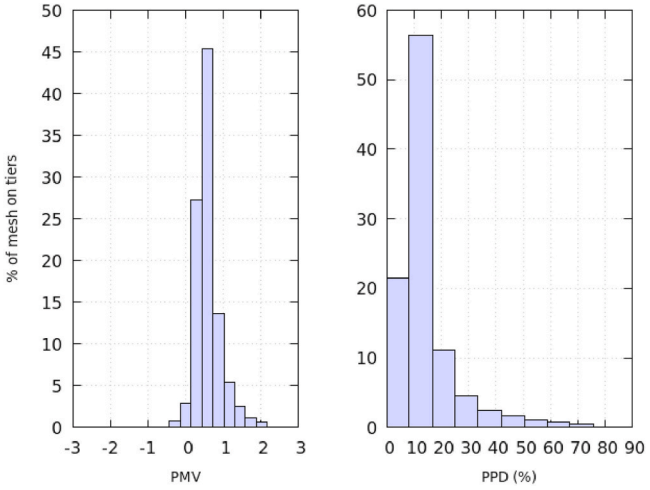

Fig. 18. Distributions of PMV and PPD indices in SIM06.

4. Conclusions

A satisfactory thermal sensation within a stadium is a prerequisite for the safe execution of the match and comfort of the occupants. Further difficulties arise in hot and humid climates, where a comprehensive analysis of the interaction between the stadium and the environment and how it affects the indoor comfort level becomes crucial for the safety of the players and spectators.

We presented a CFD-assisted analysis of the thermal comfort in a stadium designed for international football competitions. The case study was of the 2022 FIFA World Cup, which will be hosted in Doha, Qatar, a country with a hot and humid climate. To guarantee the thermal comfort of the spectators and the safety of players, we proposed a tool that assesses the thermal sensation in all stadium zones, given the climatic variations and duty cycle of the air conditioning system.

A steady-state, conjugate heat transfer model simulated the heat and mass exchanges between the stadium and the environment. The model takes into account the vapor fraction transport, buoyancy effects, turbulence, and solar radiation. The PMV and PPD indices signified the thermal comfort of the spectators in the stadium bowl, a semi-closed environment controlled by a centralized HVAC system. The analysis of the WBGT on the pitch verified that the risk of thermal stress to the players was within the safety level given by the FIFA technical guidelines. By varying the operating conditions, six simulations were performed to investigate the effects of the external air temperature and relative humidity on the indoor thermal sensation. The effects of the operating conditions of the air conditioning system were also examined. In particular, SIM06 calculated the thermal comfort under extreme conditions, when the external temperature was 48 $^{\circ}$C, and the relative humidity was 60%.

The results of SIM02 illustrated the quality of the model predictions and the interactions between the stadium and the environment. The motion of air and its stratification in the whole domain (both indoor and outdoor spaces) are simultaneous effects of the wind flow, the incident solar radiation, the presence of spectators, and the air supplied by the HVAC system. The results of the first simulation set, SIM01-SIM02-SIM03, demonstrated that the HVAC system maintained thermal neutrality at all levels of the tiers for several climatic conditions: the PMV was approximately zero with a deviation of $\pm$ 5%, the PPD was approximately 5%, and the average WBGT on the football pitch was 24$^{\circ}C$, which were well within the limits recommended in the FIFA guidelines for thermal risk. SIM04 and SIM05 investigated the effects of reducing the cooling load. When the inlet flow rate of the HVAC decreased by 50%, there was an acceptable percentage of dissatisfied persons on all tiers (the most frequent value of the PMV was 0.9 and PPD varied between 15% – 20%). The thermal risk on the pitch increased, but it remained within the safety limit; the average WBGT remained below the 30$^{\circ}C$ limit and only in some spots did it increase up to 32$^{\circ}C$. Under the most severe climate conditions (SIM06), the HVAC guarantees a satisfactory comfort level in the entire stadium (PMV varied between 0.4 – 1) except at the highest tier, where it was high at 2 (an uncomfortably warm sensation) and the PPD was between 70% – 80%. The pitch did not present a risk of thermal injury to the players because it remained below the maximum WBGT of $<$ 30$^{\circ}C$. Finally, the Givoni diagram presented the quality of thermal comfort in all the different zones of the tiers. All points (i.e., simulation results) fell within the ventilated comfort zone. According to the climate and the target cooling temperature of the pitch, they were in the winter and summer comfort zones. This diagram could guide the design of the cooling system and the assignment of the operating temperature and humidity according to the specific needs of each zone. All the results demonstrated that the designed air distribution system scarcely covered the highest level near the roof, where the hot wind entered the stadium bowl. A supplementary cooling system, installed at this upper level and used under extreme conditions, could be a suitable solution.

The proposed methodology can contribute to a quantitative description of the climate comfort in stadiums, and in general, at outdoor and semi-outdoor spaces, for which theoretical models encounter

the most difficulties because of the requirement to consider the interaction between the building and the environment.

Future developments will overcome the limitations of the current work. The upgrading of the current steady-state solver to a transient-state solver will allow the calculation of the thermal comfort indicators on a customized time-interval (e.g., from a preparatory phase to the entire duration of the match), taking into account the hourly variation of the solar radiation and wind speed. Furthermore, a transient model can check the thermal comfort of all daily activities within the building complex, including in spaces such as stores, offices, and dressing rooms. We neglected the latter in our model to focus on the thermal comfort on the pitch and the tiers. Finally, the coupling of this CFD analysis to the energy and exergy analysis of the air conditioning can help optimize the energy use and economic costs of the HVAC system.

CRediT authorship contribution statement

Gianluca Losi: Methodology, Software, Writing - original draft. **Arianna Bonzanini:** Methodology, Software, Writing - original draft. **Andrea Aquino:** Formal analysis, Writing - original draft, Writing - review & editing. **Pietro Poesio:** Supervision, Project administration.

Declaration of competing interest

The authors declare that they have no known competing financial interests or personal relationships that could have appeared to influence the work reported in this paper.

Acknowledgments

This research did not receive any specific grant from funding agencies in the public, commercial, or not-for-profit sectors. The authors would like to thank the reviewers for their insightful comments, which have resulted in an improved manuscript.

References

[1] M. Ucuncu, D. Woolf, M. Zikri, Thermal Comfort of Spectators in Stadia Built in Hot Climates, Adapting to Change: New Thinking on Comfort, Windsor, UK, 2010, p. 8.
[2] L. Shi, R. An, An optimization design approach of football stadium canopy forms based on field wind environment simulation, Energy Procedia 134 (2017) 757–767.
[3] K. Özgünen, S. Kurdak, R. Maughan, C. Zeren, S. Korkmaz, Z. Yazıcı, G. Ersöz, S. Shirreffs, M. Binnet, J. Dvorak, Effect of hot environmental conditions on physical activity patterns and temperature response of football players, Scand. J. Med. Sci. Sports 20 (2010) 140–147.
[4] J.R. Brotherhood, Heat stress and strain in exercise and sport, J. Sci. Med. Sport 11 (1) (2008) 6–19.
[5] Accuweather, [link]. URL 2019. https://www.accuweather.com/en/qa/doha/271669/july-weather/271669?.
[6] National Oceanic and Atmospheric Administration, [link]. URL 2019. https://www.noaa.gov/.
[7] M. Manni, A. Petrozzi, V. Coccia, A. Nicolini, F. Cotana, Investigating alternative development strategies for sport arenas based on active and passive systems, J. Build. Eng. (2020) 101340.
[8] J. Spagnolo, R. De Dear, A field study of thermal comfort in outdoor and semi-outdoor environments in subtropical sydney Australia, Build. Environ. 38 (5) (2003) 721–738.
[9] L. Jin, Y. Zhang, Z. Zhang, Human responses to high humidity in elevated temperatures for people in hot-humid climates, Build. Environ. 114 (2017) 257–266.
[10] S. Coccolo, J. Kämpf, J.-L. Scartezzini, D. Pearlmutter, Outdoor human comfort and thermal stress: a comprehensive review on models and standards, Urban Clim. 18 (2016) 33–57.
[11] M. Arnesano, G. Revel, F. Seri, A tool for the optimal sensor placement to optimize temperature monitoring in large sports spaces, Autom. ConStruct. 68 (2016) 223–234.
[12] T. Goto, J. Toftum, R. de Dear, P.O. Fanger, Thermal sensation and thermophysiological responses to metabolic step-changes, Int. J. Biometeorol. 50 (5) (2006) 323–332.
[13] C. Eiracle, Soccer injuries on the road to the World Cup Qatar 2022: main obstacles and challenges, J. Sci. Med. Sport 16 (1) (2013) e53–e54.
[14] M. Nikolopoulou, N. Baker, K. Steemers, Thermal comfort in outdoor urban spaces: understanding the human parameter, Sol. Energy 70 (3) (2001) 227–235.
[15] P. Sofotasiou, B.R. Hughes, J.K. Calautit, Qatar 2022: Facing the FIFA World Cup climatic and legacy challenges, Sustain. Cities Soc. 14 (1) (2015) 16–30.
[16] D.H. Kang, P.H. Mo, D.H. Choi, S.Y. Song, M.S. Yeo, K.W. Kim, Effect of mrt variation on the energy consumption in a pmv-controlled office, Build. Environ. 45 (9) (2010) 1914–1922.
[17] L. Zampetti, M. Arnesano, G. Revel, Experimental testing of a system for the energy-efficient sub-zonal heating management in indoor environments based on pmv, Energy Build. 166 (2018) 229–238.
[18] D.-S. Lee, E.-J. Kim, Y.-H. Cho, J.-W. Kang, J.-H. Jo, A field study on application of infrared thermography for estimating mean radiant temperatures in large stadiums, Energy Build. 202 (2019) 109360.
[19] E. Enríquez, V. Fuertes, M. Cabrera, J. Seores, D. Muñoz, W. More, J. Fernández, Model to evaluate the thermal comfort factor: dynamic measurement of heat flow in building materials, J. Build. Eng. 20 (2018) 344–352.
[20] J. Bouyer, J. Vinet, P. Delpech, S. Carre, Thermal comfort assessment in semi-outdoor environments: application to comfort study in stadia, J. Wind Eng. Ind. Aerod. 95 (9–11) (2007) 963–976.
[21] P. Höppe, Different aspects of assessing indoor and outdoor thermal comfort, Energy Build. 34 (6) (2002) 661–665.
[22] A. Szucs, S. Moreau, F. Allard, Aspects of stadium design for warm climates, Build. Environ. 44 (6) (2009) 1206–1214.
[23] S. Nada, H. El-Batsh, H. Elattar, N. Ali, Cfd investigation of airflow pattern, temperature distribution and thermal comfort of ufad system for theater buildings applications, J. Build. Eng. 6 (2016) 274–300.
[24] T. Van Hooff, B. Blocken, M. Van Harten, 3d cfd simulations of wind flow and wind-driven rain shelter in sports stadia: influence of stadium geometry, Build. Environ. 46 (1) (2011) 22–37.
[25] T. Uchida, R. Araya, et al., Practical applications of the large-eddy simulation technique for wind environment assessment around new national stadium, Japan (tokyo olympic stadium), Open J. Fluid Dynam. 9 (2019) 269 04.
[26] A. Palmowska, B. Lipska, Experimental study and numerical prediction of thermal and humidity conditions in the ventilated ice rink arena, Build. Environ. 108 (2016) 171–182.
[27] A. Limane, F. H, N. Galanis, Three-dimensional OpenFOAM simulation to evaluate the thermal comfort of occupants, indoor air quality and heat losses inside an indoor swimming pool, Energy Build. 167 (2018) 49–68.
[28] I.A. Stamou, I. Katsiris, A. Schaelin, Evaluation of thermal comfort in Galatsi arena of the Olympics “Athens 2004” using a CFD model, Appl. Therm. Eng. 10 (2008) 1206–1215.
[29] ANSYS CFX-Solver Manager User’s Guide, [link]. URL 2019. http://read.pudn.com/downloads500/ebook/2077964/cfx_solv.pdf.
[30] S. Ghani, E.A. ElBialy, F. Bakochristou, S.M.A. Gamaledin, M.M. Rashwan, B. Hughes, Thermal performance of stadium’s Field of Play in hot climates, Energy Build. 139 (2017) 702–718.
[31] UEFA stadium infrastructure regulation, [link]. URL 2019. https://it.uefa.com/MultimediaFiles/Download/uefaorg/Stadium&Security/01/48/48/85/1484885_DOWNLOAD.pdf.
[32] weather2visit, [link]. URL 2019. https://www.weather2visit.com/middle-east/qatar/doha-december.htm.
[33] P. Sosnowski, A. Petronio, V. Armenio, Numerical model for thin liquid film with evaporation and condensation on solid surfaces in systems with conjugated heat transfer, Int. J. Heat Mass Tran. 66 (2013) 382–395.
[34] D.M. Hargreaves, N.G. Wright, On the use of the k-ω model in commercial CFD software to model the neutral atmospheric boundary layer, J. Wind Eng. Ind. Aerod. 95 (5) (2007) 355–369.
[35] ASHRAE, Handbook of Fundamentals.
[36] J. Luo, D. N. O'Sullivan, A. Jackson, Assessing Thermal Comfort and Performance of the Airfloor Hvac System Using Multi-Software Coupled Modelling Method.
[37] C. Mannion, H. Melvin, M. Geron, M. Keane, Analysis of User Comfort and Thermal Behaviour of a Room under Forced Convection Conditions, Research Day, 2013 Schedule 37.
[38] B. Blocken, C. Gualtieri, Ten iterative steps for model development and evaluation applied to computational fluid dynamics for environmental fluid mechanics, Environ. Model. Software 33 (2012) 1–22.
[39] J. Franke, A. Hellsten, H. Schlünzen, B. Carissimo, Best Practice Guideline for the CFD Simulation of Flows in the Urban Environment, vol. 44, 2007.
[40] S. Kato, S. Murakami, T. Takahashi, T. Gyobu, Chained analysis of wind tunnel test and CFD on cross ventilation of large-scale market building, J. Wind Eng. Ind. Aerod. 67–68 (1997) 573–587.
[41] P. Karava, T. Stathopoulos, A.K. Athienitis, Wind-induced natural ventilation analysis, Sol. Energy 81 (1) (2007) 20–30.
[42] T. Van Hooff, B. Blocken, On the effect of wind direction and urban surroundings on natural ventilation of a large semi-enclosed stadium, Comput. Fluid 39 (7) (2010) 1146–1155.
[43] B. Blocken, T. Stathopoulos, J. Carmeliet, CFD simulation of the atmospheric boundary layer: wall function problems, Atmos. Environ. 41 (2) (2007) 238–252.
[44] Qatar Meteorology Department, [link]. URL 2017. http://qweather.gov.qa/index.aspx.
[45] W.L. Cheng, A. Saleem, R. Sadr, Recent warming trend in the coastal region of Qatar, Theor. Appl. Climatol. 128 (1–2) (2017) 193–205.
[46] BSI, Bs en iso 7730, Ergonomics of the Thermal Environment. Analytical Determination and Interpretation of Thermal Comfort Using Calculation of the Pmv and Ppd Indices and Local Thermal Comfort Criteria, 2005 2005.
[47] F. Fantozzi, G. Lamberti, Determination of thermal comfort in indoor sport

facilities located in moderate environments: an overview, Atmosphere 10 (12) (2019) 769.
[48] ASHRAE, Handbook of Fundamentals, Chapters 5 and 7.
[49] F. Nicol, M. Humphreys, S. Roaf, Adaptive Thermal Comfort: Principles and Practice, Routledge, 2012, pp. 10–22.
[50] R. De Dear, G. S. Brager, Developing an Adaptive Model of Thermal Comfort and Preference.
[51] R. de Dear, J. Xiong, J. Kim, B. Cao, A Review of Adaptive Thermal Comfort Research since 1998, Energy and Buildings, 2020 109893.
[52] J.F. Nicol, M.A. Humphreys, Adaptive thermal comfort and sustainable thermal standards for buildings, Energy Build. 34 (6) (2002) 563–572.
[53] ASHRAE, Standard 55: Thermal Environmental Conditions for Human Occupancy.
[54] ASHRAE, Standard 55: Thermal Environmental Conditions for Human Occupancy.
[55] C. S. EN15251, et al., Indoor Environmental Input Parameters for Design and Assessment of Energy Performance of Buildings Addressing Indoor Air Quality, Thermal Environment, Lighting and Acoustics, Thermal Environment, Lighting and Acoustics, European Committee for Standardization, Brussels.
[56] T. C. C. 156, Energy performance of buildings–part 1: indoor environmental input parameters for design and assessment of energy performance of buildings addressing indoor air quality, thermal environment, lighting and acoustics, Module M1–6 (EN 16798–1).
[57] A. Van der Linden, A.C. Boerstra, A.K. Raue, S.R. Kurvers, R. De Dear, Adaptive temperature limits: a new guideline in The Netherlands: a new approach for the assessment of building performance with respect to thermal indoor climate, Energy Build. 38 (1) (2006) 8–17.
[58] A.C. Boerstra, J. van Hoof, A. Van Weele, A new hybrid thermal comfort guideline for The Netherlands: background and development, Architect. Sci. Rev. 58 (1) (2015) 24–34.
[59] B. Li, R. Yao, Q. Wang, Y. Pan, An introduction to the Chinese evaluation standard for the indoor thermal environment, Energy Build. 82 (2014) 27–36.
[60] T.E. Bernard, Prediction of workplace wet bulb global temperature, Appl. Occup. Environ. Hyg 14 (2) (1999) 126–134.
[61] FIFA, [link]. URL 2017. http://fifamedicinediploma.com/topic/environment-temperature-measurement/.
[62] R. Stull, Wet-bulb temperature from relative humidity and air temperature, J. Appl. Meteorol. Climatol. 50 (2011) 2267–2269.
[63] V.E. Dimiceli, S.F. Piltz, S.A. Amburn, Estimation of Black Globe Temperature for Calculation of the Wet Bulb Globe Temperature Index, WCECS 2011, World Congress on Engineering and Computer Science, San Francisco, USA, 2011 2011.
[64] B. Givoni, Comfort, climate analysis and building design guidelines, Energy Build. 18 (1992) 11–23.
[65] J.L.J. Liang, R.D.R. Du, Thermal comfort control based on neural network for HVAC application, Proceedings of 2005 IEEE Conference on Control Applications, 2005, CCA 2005, 2005, pp. 819–824.